Jurnal Teknologi, 47(F) Keluaran Khas, Dis. 2007: 1–12

TANGENTIAL FLOW MICROFILTRATION OF GASIFICATION POWER PLANT EFFLUENT BY INORGANIC MEMBRANE

S. MAHESH KUMAR[1*], P. AGRAWAL[2] & S. ROY[3]

Abstract. In the present paper, treatment of gasification power plant effluent from gas scrubber was carried out using micro-porous alumina membrane tubes consisting of different channels (1 and 7) under simulated process conditions of temperature (45 – 55°C) and at varying transmembrane pressure drop (0.2 – 2 bar). The effect of membrane geometry on the membrane separation characteristics and fouling behavior was studied. The experimental results show that the flux decreases significantly (~ 40%) during the first few minutes (10 min) of filtration which then stabilized with time. This behavior can be attributed to the classical dependence of flux on the time in microfiltration, which shows development of a relatively important fouling layer on the membrane surface. The characteristics of the effluent after filtration showed significant decrease in turbidity (95%), COD (50%), total dissolved solids (10%), and total solids (55%). The total suspended solids are reduced by almost 100% and the pH remained unchanged (in the field of neutrality) during the process. The effect of various resistances that are acting in series was calculated using Darcy's Law. These experimental results indicated that different filtration laws could be applied simultaneously for the description of the filtration data, which were found during cross-flow microfiltration of gasification power plant effluent.

Keywords: Ceramic membrane, gasification effluent, microfiltration, fouling, membrane cleaning

1.0 INTRODUCTION

Biomass gasification, a century old technology, is viewed today as an alternative to conventional fuel. Gasification is basically a thermo-chemical process, which converts biomass (wood & charcoal) materials into gaseous component. The result of gasification is the producer gas, containing carbon monoxide, hydrogen, methane and some inert gases. If complete gasification takes place, all the carbon is burnt or reduced to carbon monoxide, a combustible gas and some other mineral matter is vaporized. The remains are ash and some char (unburned carbon) [1]. Mixed with air, the producer gas can be used as gasoline or in diesel engine with little modifications.

In a typical gasification plant, water is used for cooling and scrubbing of the gas, which is emitted out of the gasifier section. Almost all the impurities present in the producer gas will be carried away by the water during the scrubbing process. This

[1&2]Department of Biotechnology, RVCE, Bangalore – 560 059, India
[3] Ceramic Technology Institute, EPD, BHEL, Bangalore – 560 012, India
[*] *Corresponding author*: GE, John F Welch Technology Center, Bangalore – 560066, +9180-40120466. Email: smahesh.kumar@ge.com

process leads to the generation of effluent water which is mainly composed of suspended solids (low density), amines, sulphides, cyanides, phenolic compound, phosphates and other trace impurities [1]. Conventionally, effluent treatment incorporates physical, chemical and biological processes which treats and removes physical, chemical and biological contaminants from water. The objective of the treatment is two fold, first to produce clean waste stream (treated effluent) suitable for discharge or reuse back into the process, and secondly a solid waste or sludge also suitable for proper disposal or reuse. The level of pollution in the gasification power plant effluent coupled with regulatory pressure is challenging societies to find feasible management strategies and treatment alternatives of the effluent.

With the recent growing awareness of membrane filtration and declining cost of membranes, the use of membrane microfiltration within the gasification power plant may be a viable management and treatment option for many gasification power plant installations. Typical advantages of microfiltration membranes include reduced land requirements compared to sediment tanks, ability to reject suspended solids, bacteria, decrease turbidity and BOD.

Of late, ceramic membranes are receiving greater attention because of their advantages over polymeric and metallic membranes. Compared to polymeric based membranes, ceramic membranes exhibit unquestionable advantages [2], due essentially to their inherit properties. They can withstand high temperatures, high pressure (>100 bar), abrasion, and chemical attack. Recent studies have showed that ceramic membranes exhibits high stability against microbiological attack [3]. Generally, they are stable up to 1000°C, which enable them for high-temperature applications and can be sterilized. Ceramic membranes can tolerate chemical/mechanical cleaning, can readily accommodate the abrasion encountered in slurries, and resist the build up of high pressure (up to 30 atm) often used in back flushing techniques for membrane cleaning [4].

Although the inorganic membrane based microfiltration technology has long been popular in the waste water treatment processes [5-8], it has been rarely employed for the direct treatment of gasification power plant effluent. In fact literature pertaining to treatment of gasification power plant effluent is very rare.

This research work focused on inorganic membrane filterability corresponding to various operational parameters. For this, tubular monolithic microporous ceramic membranes with different geometry were selected for the treatment studies of gasification power plant effluent. The key operational and design parameters for cross-flow microfiltration like permeate flux rate, transmembrane pressure, resistance to flow and operating temperature as a function of effluent quality were examined.

2.0 MATERIALS AND METHODS

2.1 System Description

A bench-scale cross-flow ceramic membrane filtration module used in the present work is represented in Figure 1. The module consisted of a 1.5 HP centrifugal pump with a variable frequency drive, a 15-L feed tank with a water jacket for temperature control, a ceramic test module housing one membrane, a thermowell, eight process control diaphragm valves, and four pressure gauges to monitor the bypass, inlet, outlet and permeate pressure. The filtration system was designed to achieve a cross flow velocity of 5 m/s to 10 m/s. The experiments were performed with a transmembrane pressure between 0.3 and 1.45 bar and at a constant temperature of 26 ± 2°C. The cross-flow through the membrane module was controlled by regulating the pump.

Gasification power plant effluent directly from the plant was collected in a 25 l plastic container and was used without any storage. The characteristics of effluent before and after filtration were analyzed by standard methods discussed elsewhere [9]. The physical and chemical characteristics of the effluent are presented in Table 1.

For the present work 2 tubular α-alumina ceramic membrane with a mean pore diameter of 1.2 μm were used. Each tubular membrane was 520 mm in length and 30 mm in diameter, but one was of tubular type with an effective surface area of 0.04 m^2 and the other was a monolith type of 7 channels each of diameter 5.5 mm with an effective surface area of 0.063 m^2. Both the membranes are capable of withstanding a pressure limit of 10 bar, a temperature limit of 255°C and are stable between the pH of 0 – 14.

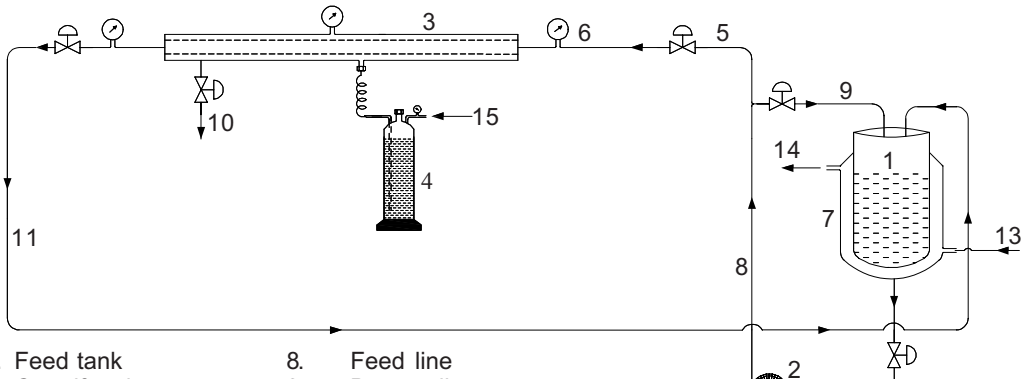

1. Feed tank
2. Centrifugal pump
3. Membrane module
4. Back pulsing unit
5. Diaphragm valve
6. Pressure gauges
7. Jacket
8. Feed line
9. Bypass line
10. Permeate line
11. Retentate line
12. Drain
13. Cold water in
14. Cold water out
15. Compressed N_2 inlet

Figure 1 Schematic representation of experimental set up

2.2 Calculation of Permeate Data and Membrane Resistance

Permeate and time data were periodically collected during each experiment. The permeate flux rate was calculated using Equation (1). The permeate fluxes were then analyzed using classical filtration theory as described elsewhere [10].

$$J = \frac{dV}{dt}\left(\frac{1}{A_m}\right) \tag{1}$$

Where J is the transient permeate flux, dV is the differential volume, dt is the differential time and A_m is the effective membrane surface area. After each run, the membrane module was first washed with tap water for 5 min and then it was thoroughly cleaned using 0.01 N (2%) sodium hydroxide (NaOH) solution, followed by rinsing extensively with distilled and de-ionized water.

The characteristics of membrane fouling were evaluated based on the resistance-in-series model. According to this model the permeate flux and the membrane resistances can be expressed as per the following equations.

$$J = \Delta P/(\mu.R_t) \tag{2}$$

$$R_t = R_m + R_f \tag{3}$$

$$1/J_w = (\mu/\Delta P) * R_m \tag{4}$$

$$1/J_w^1 = (\mu/\Delta P) * (R_m + R_f) \tag{5}$$

J_w is the initial pure water flux of the membrane, while J_w^1 is the pure water flux after cleaning the membrane; ΔP is the transmembrane pressure (Pa); μ is the dynamic viscosity of the permeate (Pa.s); R_t is the total resistance (m^{-1}); R_m is membrane resistance (m^{-1}); R_f is the plugging layer resistance due to some colloidal adsorption (m^{-1}) and R_r is the external fouling resistance formed by a strongly deposited cake layer on the membrane surface (m^{-1}). These equations were used to calculate the values of each resistance term of the membrane.

3.0 RESULTS AND DISCUSSIONS

The effects of various operating parameters on permeate quality and filtration characteristics, like membrane fouling, membrane and fouling resistance, flux decline, membrane blocking, back pulsing, cleaning etc during cross flow microfiltration of gasification power plant effluent was studied. Experiments were conducted using two ceramic membranes having same physical and chemical characteristics but with different geometry. The pore size and the apparent porosity of the two membranes were 1.2 μm and 45% respectively.

3.1 Effect of Transmembrane Pressure (TMP) on Flux of Water and Gasification Effluent

The effects of TMP on permeate flux for distilled water and gasification power plant effluent for both membrane configurations are represented in the Figure 2. As seen from the figure the flux of the water increases linearly with TMP but in case of the effluent it increases linearly till 1.75 bar and thereafter it remain constant, which indicates that increase in TMP have negligible effect on the effluent flux. For single channel membrane configuration (membrane area = 0.04 m^2), the flux is relatively high when compared to the seven channel membrane configuration (membrane area = 0.063 m^2) due to increase in area and channels, which offers resistance for the flow. Hence operating at TMP of 1.75 will be optimum to obtain high flux. But, the quality of permeate is know to vary with TMP and hence the effect of TMP on the permeate quality should also be investigated before any conclusions.

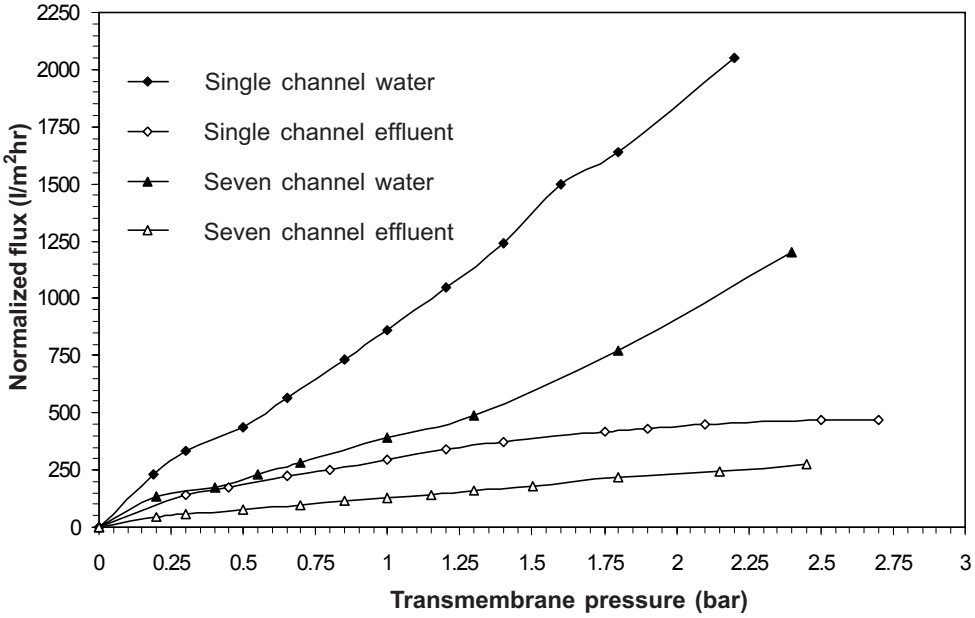

Figure 2 Effect of transmembrane pressure on flux, at 30°C, for membranes with pore size of 1.2 μm

3.2 Effect of Transmembrane Pressure on Permeate Quality

The effect of permeate quality at varying TMP was investigated for both the membrane configuration at constant temperature of 30°C. Table 1 represents the characteristics of the gasification power plant effluent before and after filtration. The quality of the permeate decreases with increase in TMP. This phenomenon was observed for both membrane configurations, however, with respect to seven channel membrane configuration the

permeate quality was relatively better as compared to single channel membrane configuration. This can be attributed to the increased membrane area as the feed pass through the barrier twice before it enters the permeate line. This leads to improved rejection by the membrane. At high feed pressures, the solids in the feed force itself to permeate through the pore thereby leading to decreased permeate quality and pore blocking. One of the interesting finding in the present investigations was that decreased conductivity which is mainly due to adsorption of the inorganic ions on alumina membrane. This observation can be viewed as advantages as well as limitations for the application of mineral (ceramic) membranes for the effluent treatment processes. These membranes can be effective in reducing conductivity (TDS) of the effluent water but with increase process time, the membranes becomes saturated and can also lead to pore blocking, leading to increased operating and maintenance cost. Hence more experimental trials need to be carried out to understand the filtration mechanism.

Table 1 Characteristics of gasification power plant effluent before and after filtration, at 30°C

Characteristics		Feed	Single channel			Seven channel		
			TMP=0.3	TMP=0.7	TMP=1.2	TMP=0.3	MP=0.7	TMP=1.2
Total solids (mg/lt)	Max.	1820	790	810	820	765	775	780
	Min.	1570	605	615	630	580	587	595
	Avg.	1695	698	713	725	673	681	688
Total dissolved solids (mg/lt)	Max.	880	790	802	810	760	773	780
	Min.	620	590	605	620	575	585	595
	Avg.	750	690	703	715	668	679	688
Total suspendable solids (mg/lt)	Max.	990	4	4	4	4	4	4
	Min.	900	0	0	0	0	0	0
	Avg.	945	2	2	2	2	2	2
Conductivity ($\mu s/cm^2$)	Max.	2450	1850	1850	1900	1350	1360	1375
	Min.	2355	1700	1725	1750	1260	1305	1310
	Avg.	2400	1770	1805	1835	1295	1330	1350
Turbidity (NTU)	Max.	90	5	5	5	5	5	5
	Min.	78	3	3	3	3	3	3
	Avg.	84	4	4	4	4	4	4
Chemical Oxygen Demand (mg/lt)	Max.	660	360	375	380	346	360	360
	Min.	375	136	150	163	55	60	67
	Avg.	518	248	263	271	201	210	213
Biological Oxygen Demand (mg/lt)	Max.	244	112	112	122	104	109	109
	Min.	215	91	97	100	78	78	98
	Avg.	224.5	104	106	114	90	98	105

3.3 Analysis of Filtration Curves

Analysis of the filtration mechanisms using the general expression for the filtration laws [10] showed that, the filtration mechanism followed three stages, namely, cake formation, cake filtration, and cake filtration with compression (Figures 3 and 4). In

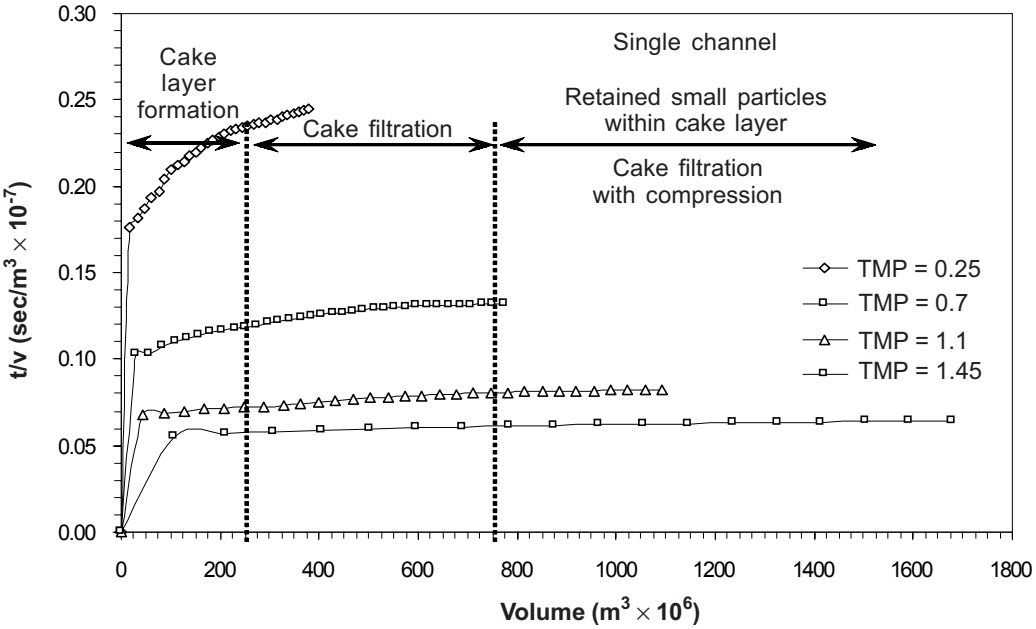

Figure 3 Plot of ratio of filtration time and filtration volume as a function total volume of filtrate at different TMP for single channel membrane configuration at 30°C

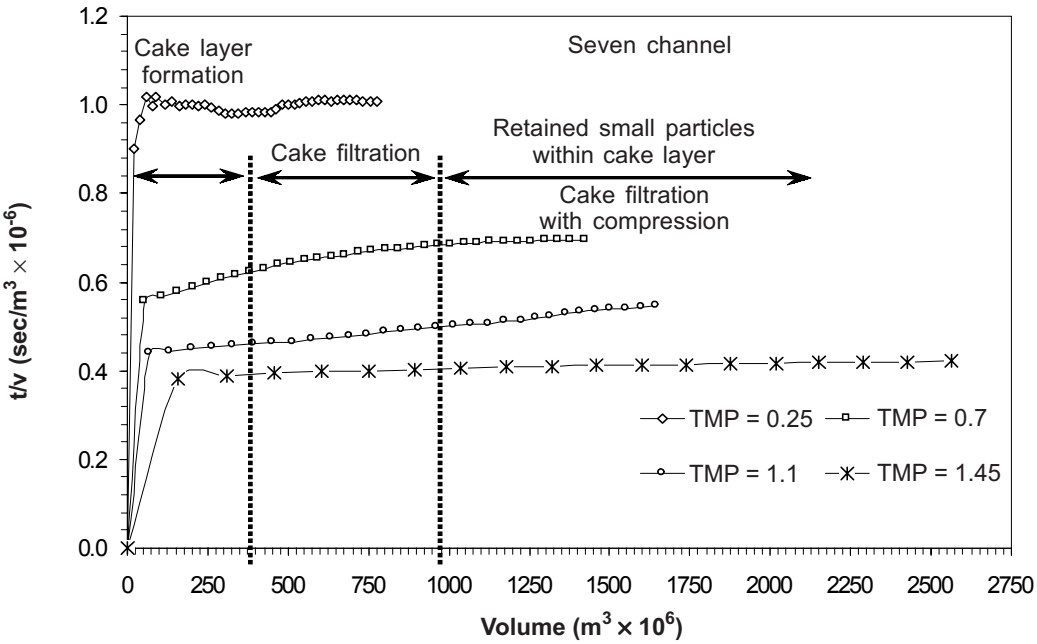

Figure 4 Plot of ratio of filtration time and filtration volume as a function total volume of filtrate at different TMP for seven channel membrane configuration at 30°C

the present case, the filtration curve was mainly influenced by the growing layer of the compressible cake (solid deposition) on top of the membrane surface. At higher TMP, the formation of cake over the surface of the membrane was rapid and then stabilized over the entire filtration process. The same profile was observed for both membrane configurations. This might be due to the high driving force (TMP) acting on the feed components. In the first few minutes of the filtration cycle, a constant layer of cake was formed (boundary layer) over the membrane surface followed by cake filtration. For single channel membrane configuration, cake filtration with cake compression started at a relatively faster rate compared to seven channel membrane configuration. This can be due to increased barrier where the deposition of the solid particles on the membrane surface is distributed over the seven channels.

3.4 Flux Decline Phenomenon

The effect of time on flux was studied for both the membrane configuration at varying transmembrane pressures and at constant temperature of 30°C for approximately 18 min.

From Figure 5 it is evident that at high TMP (>1.1 bar), the rate of flux decline is higher than at lower TMP. This is due to increase in tangential forces acting on the solid particles that are present in the feed stream. Hence carrying filtration process at TMP less than 1 bar would be favorable to obtain optimum flux and permeate quality.

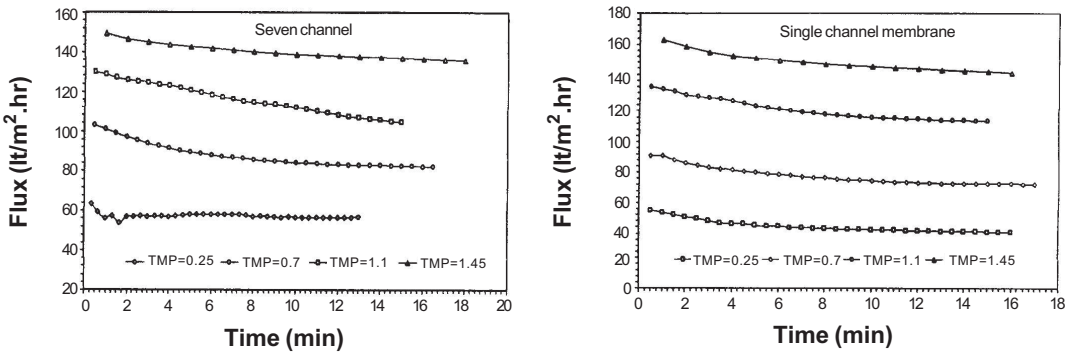

Figure 5 Plot of flux with respect to time for various TMP at 30°C

3.5 Effect of Various Membrane Resistances Affecting Flux

Total membrane resistance (R_t) affecting the permeate flux at varying TMP was also investigated and was found that with pressure the resistance increases rapidly during the first few minutes of the filtration process and later stabilizes with time. At low TMP the total membrane resistance increases linearly with time during the filtration processes and took a longer time for stabilization. The same profile was observed for both membrane configurations. But from the Figure 6, it was observed that the total resistance

at a TMP of 1.1 is negligibly higher compared to that at TMP of 1.45. This can be attributed to the formation of a constant fouling layer on the membrane surface which maintains a constant boundary layer at high pressures (>1.2). The membrane fouling layer resistance (R_f) for both the membrane configuration are represented in Figure 7. The same profile of the graph was observed in this case and the above explanation holds good for this case also.

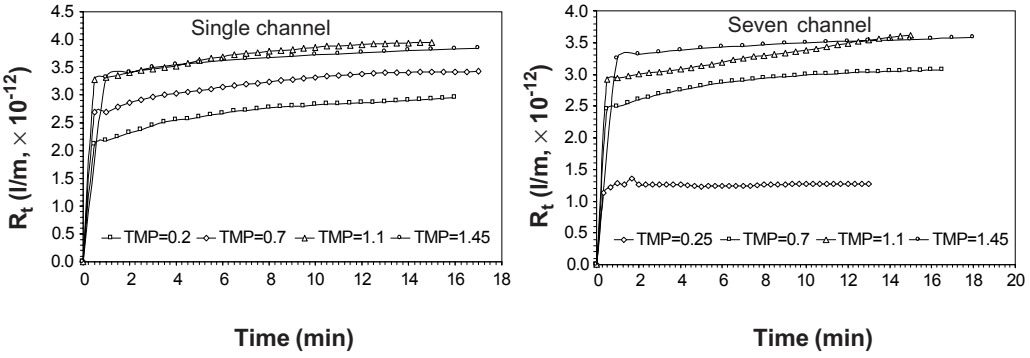

Figure 6 Plot of total membrane resistance versus time at 30°C and at various pressures

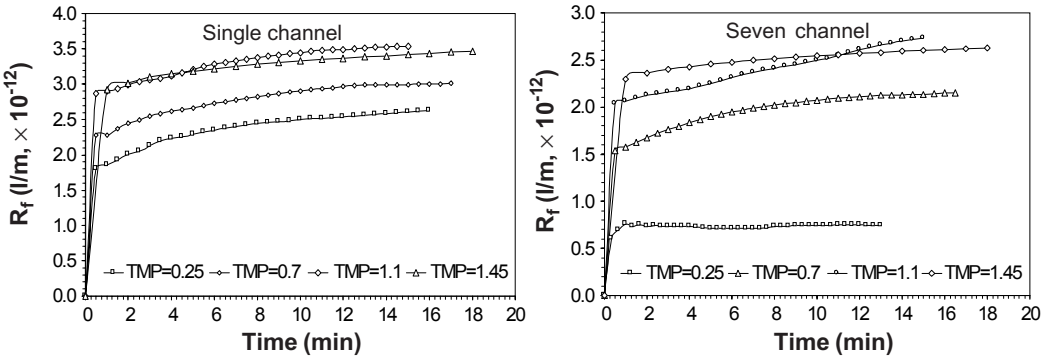

Figure 7 Plot of membrane fouling layer resistance versus time at 30°C and at various pressures

3.6 Validation of the Filtration Mechanism

Firstly, the relationship between time (t) and filtered volume (V) was drawn for all the TMP. In all, the volume of permeate linearly increased with time. In the analysis of the filtration mechanism, the first 5 minutes of filtration process was neglected in order to achieve steady state conditions. The models that were defined by Hermia [10] for the description of various filtration laws were applied to permeate flux data that were obtained in the current studies. Linear relationship of t/V versus V, t/V versus t, and flow rate versus filtrate volume was determined experimentally for cake filtration model (CFM), standard blocking model (SBM), and complete pore blocking model (CPBM) respectively. All the filtration data at different TMP was also calculated and fitted for

these models with calculation of the correlation coefficient R^2. For each experiment, the R^2 of the cake filtration curve, the standard blocking curve, and the complete pore-blocking curve was compared.

Figures 8, 9, and 10 represent the plot of t/V versus V, t/V versus t, and flow rate versus volume respectively. To determine whether the data agreed with any one of the models studied, regression coefficient (R^2) was compared relatively with the other two models.

For single channel membrane configuration, compared to all the plots of the models, the cake filtration model was found to fit well (regression coefficient >0.890) at all TMP with relative to the standard blocking and complete pore blocking models. The lower linear coefficient (0.870 – 0.932) in the latter two models (SBM, CPBM) indicates that although some standard blocking and complete pore blocking is occurring, the cake filtration mechanism is predominant.

For seven channel membrane configuration, compared to all the plots of the models, the cake filtration model was found to fit well (regression coefficient >0.780) at all TMP with relative to the standard blocking and complete pore blocking models. The

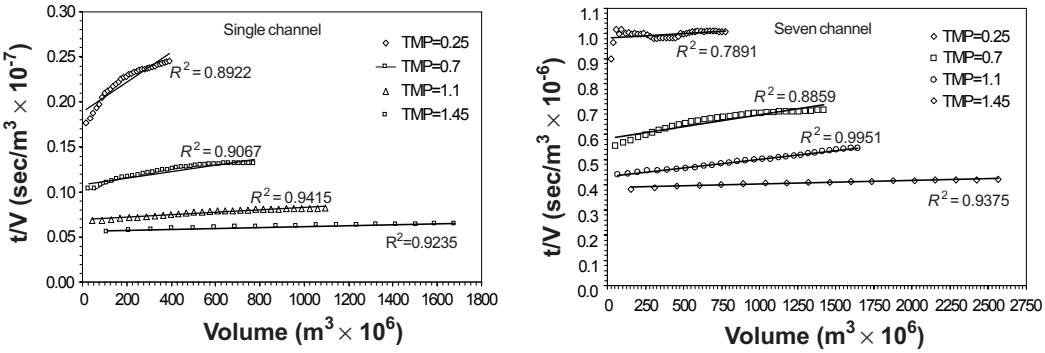

Figure 8 Plot of filtration data for gasification effluent according to Hermia cake formation model (CFM) varying TMP

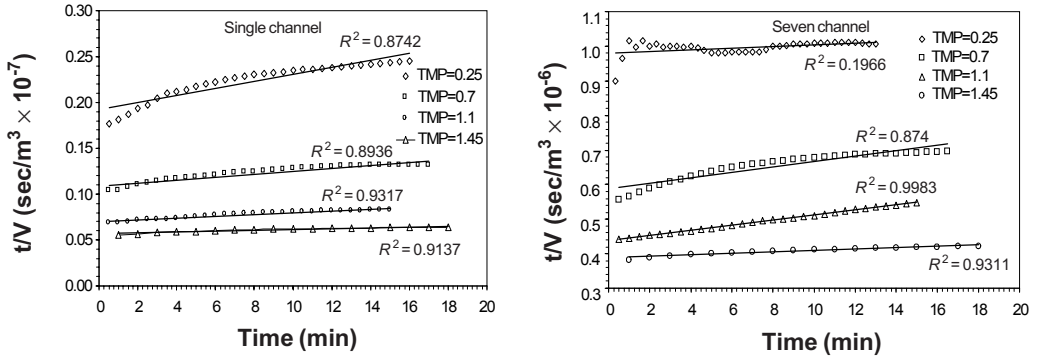

Figure 9 Plot of filtration data for gasification effluent according to Hermia standard blocking model (SBM) at varying TMP

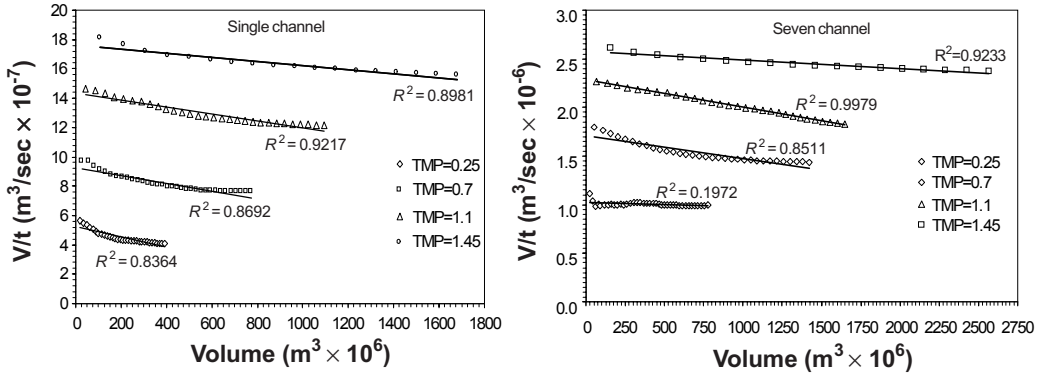

Figure 10 Plot of filtration data for gasification effluent according to Hermia complete pore blocking model (CPBM) at varying TMP

lower linear coefficient (0.200 – 0.870) in the latter two models indicates that at higher pressure the standard blocking model and complete pore blocking model predominates the cake filtration model.

However, when the linear regression coefficient for different filtration models were compared (Table 2), it was found that at lower pressures (<1 bar), there was a significant difference between in the value of the R^2 from one model to the other but at high pressure (>1) the deviation in most experiments was less than 1 – 3%. These experimental results indicate that different filtration laws could be applied simultaneously for the description of the filtration data, which were found during dead-end microfiltration of gasification power plant effluent.

Table 2 Linear regression coefficient for different blocking models at varying TMP

Linearity	R^2 - Single channel				R^2 - Seven channel			
	TMP (bar)				TMP (bar)			
	0.25	**0.7**	**1.1**	**1.45**	**0.25**	**0.7**	**1.1**	**1.45**
t/V *vs.* V	**0.892**	**0.907**	**0.942**	**0.924**	**0.789**	**0.886**	0.995	**0.938**
t/V *vs.* t	0.874	0.894	0.932	0.914	0.197	0.874	**0.998**	0.931
V/t *vs.*V	0.836	0.869	0.922	0.898	0.197	0.851	**0.998**	0.923

t/V *vs.* V is CFM, t/V *vs.* t is SBM, V/t *vs.* V is CPBM

4.0 CONCLUSIONS

On the basis of the results obtained in the present work, the main conclusions can be summarized as follows:

The steady state permeate flux was found to remain constant at a TMP greater than 1.75 bar indicating the saturation effect of TMP on permeate flux. The quality of the treated water was found to decrease marginally (<10%) with increase in TMP from 0.3 bar to 1.2 bar. The magnitude of the total membrane resistance (R_t) and fouling

membrane resistance (R_f) was found to be the same for both tubular and monolith membrane at higher TMP (>0.7bar), but at lower TMP (<0.5 bar) the monolith membrane showed less R_t and R_f when compared to tubular membrane. The fouling layer resistance contributed to about 88% and 77% of the total membrane resistance in case of tubular membrane and monolith membrane respectively. High concentration of the suspended solids in the effluent contributed to less permeation flux and increased the rate of fouling at high. The fouling trend predicted by the Hermia model agrees with the experimental data in the literature. However, analyzing filtration data only on the basis of filtration laws is not strong enough to determine the single filtration mechanisms that occur during cross-flow microfiltration of gasification effluent.

REFERENCES

[1] Netpro Renewable Energy India Pvt. Ltd. 2002. Product Report.

[2] Mahesh Kumar, S. 2004. Preparation and Evaluation of Clarification Efficiency and Stability of Microporous Alumina (Al_2O_3) Membranes. M.Tech Thesis, Department of Chemical Engg. Visvesaraya Technological University, India.

[3] Charpin, J., P. Bergez, F. Valin, H. Barnier, A. Maurel, and J. M. Martinet. 1998. Inorganic Membranes: Preparation Characterization, Specific Applications. *Ind. Ceramics*. 8: 23–27.

[4] Charpin, J. P. Bergez, and A. Maurel. 1986. Inorganic Membranes, Preparation, Characterization Separation Applications. 6th CIMTEC, Milan.

[5] Messalem, R., A. Brenner, S. Shandalov, Y. Leroux, P. Uzlaner, G. Oron, and D. Wolf. 2000. Pilot Study of SBR Biological Treatment and Microfiltration for Reclamation and Reuse of Municipal Wastewater. *Water Science and Technology*. 42(1): 263-268.

[6] Durham, B., M. M. Bourbigot, and T. Pankratz. 2001. Membranes as Pretreatment to Desalination in Wastewater Reuse: Operating Experience in the Municipal and Industrial Sectors. *Desalination*. 138: 83-90.

[7] Hoof, S. C. J. M. van, C. P. T. M. Duyvesteijn, and P. P. R. Vaal. 1998. Dead-end Ultrafiltration of Pretreated and Untreated WWTP Effluent for Re-use in Process Water Applications. *Desalination*. 118(1): 249-254.

[8] Mahesh Kumar S., P. Agrawal, and S. Roy. 2005. Fouling Mechanism of Microporous Alumina Membrane During Microfiltration of Saccharomyces Cerevisiae. Proceedings of CHEMCON. IIT Delhi. 14 – 17 December 2005.

[9] Apha, Awwa, Wef. 1995. *Standard Methods for the Examination of Water and Wastewater*. 19th ed. Washington, D.C: American Public Health Association.

[10] Hermia, J. 1982. Constant Pressure Blocking Filtration Laws - Application to Power-law Non-Newtonian Fluids. *Transactions of the Institution of Chem. Engg*. 60: 183-187.